


Bioimaging Different Color Emissive Copper Nanoclusters for Cancer Cell Imaging

Kingshuk Basu

Related papers

[Download a PDF Pack](#) of the best related papers 



[Formation of Fluorescent Metal \(Au, Ag\) Nanoclusters Capped in Bovine Serum Albumin Follo...](#)

Klaus Hollemeyer

[Protein-protected luminescent noble metal quantum clusters: an emerging trend in atomic cluster n...](#)

Kamalesh Chaudhari

[Sodium Cholate-Templated Blue Light-Emitting Ag Subnanoclusters: In Vivo Toxicity and Imaging in Z...](#)

Nagappan Rajendiran

Bioimaging

Different Color Emissive Copper Nanoclusters for Cancer Cell Imaging

Kingshuk Basu,^[a] Kousik Gayen,^[a] Tulika Mitra,^[b] Abhishek Baral,^[a] Sib Sankar Roy,^[b] and Arindam Banerjee*^[a]

Abstract: Different sized copper nanoclusters (CuNCs) have been synthesized in water from the same metal precursor and stabilizing agent, only by altering the reducing agent, temperature and pH of the medium. As-synthesized clusters were thoroughly characterized by fluorescent spectroscopy, matrix-assisted laser desorption ionization (MALDI) mass spectrometry, X-ray photoelectron spectroscopy (XPS), Fourier transform infra-red spectroscopy (FT-IR) and transmission electron microscopy (TEM). Interestingly, the emissive color of nanoclusters has been successfully tuned from blue to

orange-red in aqueous media and four different color emitting clusters have been found, namely, blue, cyan, green and orange-red. Orange-red emitting CuNC is associated with a large Stokes shift of 283 nm and it is non-cytotoxic in nature. Fluorophores with such high Stokes shift are highly advantageous for modern microscopic techniques; in this study, the as-synthesized orange-red emitting clusters have been employed for imaging of cancer cells to check their ability for cell imaging for future biomedical applications.

Introduction

Fluorescent noble metal nanoclusters (NCs) are an emerging field of research due to their excellent fluorescent properties and applications in biology and material science.^[1] Au- and Ag-derived metal NCs are relatively widely studied nanomaterials compared to Cu nanoclusters (CuNCs) due to their higher stability. Therefore, stabilization of CuNC continues to be an enigma to scientists.^[2] The lower redox stability of Cu⁰ with its lower standard reduction potential ($E_{\text{Cu}^{2+}/\text{Cu}}^0 = +0.377 \text{ V}$) compared to other members of Group 11 noble metals, like Ag and Au ($E_{\text{Ag}^+/\text{Ag}}^0 = +0.799$ and $E_{\text{Au}^{3+}/\text{Au}}^0 = +1.5 \text{ V}$),^[3] makes such tiny sized particles very reactive towards environmental conditions.^[2] However, high costs of Ag and Au noble metal precursors limit their large scale production, therefore synthesis of CuNCs is not only a challenging but also interesting research field for both scientific and industrial researchers.^[4] Nanoclusters are important also for their fascinating biological applications, hence they should have fair stability in aqueous media to serve this purpose.^[1] In this context, synthesis and

stabilization of CuNCs in an environmentally safe solvent like water is important not only to find a green synthesis route, but also for their applications in biosensing and bioimaging.^[5] Biomolecules have been attractive stabilizing agents for the synthesis of water soluble CuNCs, Wang and co-workers have recently synthesized DNA-hosted CuNCs in aqueous medium for identification of their polymorphism.^[6] Chattopadhyay and co-workers have synthesized blue fluorescent CuNCs in aqueous medium for fluorescent imaging of HeLa cells.^[7]

For metal NCs, a perfect and interesting route of emission color tuning would be to synthesize different fluorescent species with a variety of applications from the same sources.^[1] For Au- and Ag-derived nanoclusters much work has been done on the tuning of fluorescence emission. However, the synthesis of different color emissive CuNCs is a still less-addressed problem. Chen and co-workers have synthesized dual emissive CuNCs in nonpolar medium based on the modified Brust-Schiffrin method.^[8] So, there is a real need not only to find a good synthetic procedure for CuNCs in aqueous medium but also to tune the emissive color from blue to red and to apply these fluorescent materials for sensing or bioimaging. Glutathione (reduced), [γ -(L)-glutamyl-(L)-cysteinyl-glycine (GSH)] is a bioactive peptide and is found inside the cellular compartments like mitochondria, cytosol etc.^[9] Glutathione is also useful for stabilizing metal nanoclusters. Wang and co-workers have recently reported a synthetic route for glutathione stabilized CuNCs by core etching method.^[10a] Chen and co-workers have synthesized red emitting CuNC with 6 Cu atoms using glutathione as a stabilizing agent. Moreover, they have proved the presence of Cu-S bond by using spectroscopic methods.^[10b] Glutathione has been chosen by different groups as

[a] K. Basu, K. Gayen, Dr. A. Baral, Prof. A. Banerjee
Department of Biological Chemistry
Indian Association for the Cultivation of Science
2A & 2B Raja S. C. Mallick Road, Jadavpur, Kolkata-700032 (India)
E-mail: bcab@iacs.res.in

[b] T. Mitra, Dr. S. S. Roy
Cell Biology and Physiology Division
CSIR-Indian Institute of Chemical Biology
4 Raja S. C. Mallick Road, Jadavpur, Kolkata-700032 (India)

Supporting information and the ORCID identification number(s) for the author(s) of this article can be found under <https://doi.org/10.1002/cnma.201700162>.

stabilizing agent for metal nanoclusters, due to the following reasons: (a) –SH group is a good functional group for stabilizing metal ions due to the presence of two lone electron pairs and therefore, it is widely used as a stabilizing agent in metal nanomaterial synthesis^[10] and (b) being a bioactive peptide, glutathione plays an important role in storage, metabolism and transport of metal ions across the cell membrane, increasing the possibility of GSH capped clusters to enter inside the cells.^[11] Moreover it has free –NH₂ and –COOH groups in its structure to impart sufficient solubility in the nanocluster.

Many systematic studies have been performed regarding the synthesis and applications of the CuNCs. However, very few reports are available in literature that describe the tuning of emission color of the CuNCs obtained from same precursor and same stabilizing agent. Most of these studies include emission color tuning in a very narrow range.^[4c,j] Moreover, it is worth to mention that most of the CuNCs have been synthesized at very high pH range and by using various organic solvents and this is not desirable for biological applications of these nanomaterials.^[5f,i,10] Therefore, it is important to prepare multiple color emissive CuNCs in water with neutral or physiological pH. In this study, few atom CuNCs has been synthesized from same metal precursor, copper acetate monohydrate [Cu(OAc)₂, H₂O] and stabilizing agent, glutathione (GSH); only reaction temperature, pH and reducing agent were varied throughout the process. Thus, four different clusters have been found namely, blue, cyan, green and orange-red. These new fluorescent materials have been thoroughly characterized by different techniques to get an insight about their structures and applications. The Stokes' shifts associated with the CuNCs are very high. For blue, cyan and green nanoclusters the values of Stokes' shifts are 77, 11 and 127 nm, respectively. It was found that the orange-red emitting CuNC shows a Stokes shift of 283 nm, which is highest in the series. Fluorophores with such a high Stokes shift are particularly useful for fluorescent microscopy like stimulated emission depletion (STED) microscopy, where selective excitation of the fluorophore is required at the expense of other fluorophores already present inside the cell.^[12] Chattopadhyay and co-workers have also reported bioimaging applications of red emitting copper nanoclusters with a comparable high Stokes shift of 285 nm.^[2] The orange-red CuNCs show almost no cytotoxicity to the OAW42 cell line over 0–100 μg mL⁻¹. Fluorescence microscopy confirmed the uptake of nanoclusters by cells, and a bright red fluorescence was observed under the microscope. Quantum yields of blue, cyan and green emitting CuNCs have been found to be 1.24, 1.27 and 0.438%. It has been shown previously that nanoclusters stabilized with small ligands in aqueous medium generally show lower quantum yield^[5f,h,13] values compared to the nanoclusters stabilized with macromolecules, for example, proteins^[7a] and synthetic polymers.^[2,14] This probably happens due to dissipation of fluorescence excited state energy by non-radiative pathways.^[5h] Therefore, our results are comparable with the other previously reported studies in which small molecules have been used as stabilizing agents. From MALDI-TOF analysis, it has been found that the blue CuNC has a molecular formula of Cu₃(GS), the cyan one is com-

posed of two species: Cu₅(GS)₅ and Cu₉(GS)₅, whereas the green and orange red nanoclusters are composed of Cu₁₀(GS)₉ and Cu₁₃(GS)₁₃, respectively. The number of Cu atoms for all these CuNCs never exceeds 13. This observation is consistent with the previously reported work by Rivas and co-workers, which describes that only copper nanoclusters in which the number of copper atoms within the nanocluster is ≤ 13 show fluorescence.^[15] Many other groups have reported fluorescent metal clusters with Cu,^[4d] Cu₄,^[4a] Cu₆,^[4h] Cu₇,^[4i] and Cu₉^[7] metallic frameworks. XPS and FT-IR studies for the orange-red CuNCs suggest the presence of chemisorbed S atom and the absence of S–H of glutathione indicating the presence of the Cu–S bond in the cluster.

Results and Discussion

Synthetic protocol

In all cases the metal precursor was copper acetate monohydrate [Cu(OAc)₂, H₂O] and for stabilizing the nanoclusters reduced glutathione (GSH) was used (see Table S1 of Supporting Information). Many other groups have successfully used glutathione as a stabilizing agent; they have maintained a basic pH to synthesize the desired nanoclusters.^[5f,i,10b] However, in this study we have maintained almost neutral or physiological pH (7.46) to maximize the use of CuNCs as biomaterials in future. Blue, cyan and green clusters were synthesized in neutral aqueous medium and orange-red cluster was synthesized at pH 7.46. To the best of our knowledge this is the first report of tuning fluorescent emission of copper nanoclusters using glutathione as a stabilizing agent. Throughout the synthetic procedure, the amount of reactants, temperature and pH were varied in a trial and error manner. In this way, we found changes in ligand to metal ratio, temperature and pH lead to the formation of different color emissive nanoclusters. Synthetic details of the CuNCs are given in the Experimental Section and in tabulated form in the Supporting Information. Synthesis of blue CuNC needs a ligand-to-metal ratio of 2:1, a fixed temperature of 140 °C for 8 hours under nitrogen atmosphere and a strong reducing agent NaBH₄. For making of cyan CuNC the ligand to metal ratio was 1:1 and a milder reducing agent, trisodium citrate (to control the reduction kinetics) had been used keeping the reaction at 140 °C for 20 hours under nitrogenous environment. For the synthesis of green CuNC, the ligand-to-metal ratio was kept at 0.8:1 and a weak reducing agent, ascorbic acid (to control the reduction kinetics) was used keeping the reaction mixture at 120 °C for 7 hours at nitrogenous atmosphere. All above-stated reactions were carried out at elevated temperature and in Milli-Q water. However, all tricks for making red emitting clusters failed at higher temperature and at neutral condition. Formation of red CuNC required a ligand-to-metal ratio of 1:1 and a strong reducing agent NaBH₄, keeping the reaction mixture at 5 °C in an ice-water bath for one hour under nitrogen atmosphere. All the above-stated experiments were repeated 5 times to check the reproducibility of these nanoclusters.

UV/Visible spectroscopic studies

UV/Vis absorption studies for all four CuNCs show almost featureless absorption tails (Figure S1 of Supporting Information). In all cases the absorption curve rises after a certain point. However, for all the four clusters this break point does not appear at the same wavelength, for blue cluster a stiff rise of absorption intensity appears after 322 nm, whereas cyan nano-cluster shows two such break points in the corresponding spectrum, one at 320 nm and another at 406 nm. For green and red CuNCs similar rise in absorption spectrum appear after 413 and 434 nm, respectively. From these observations it can be stated that, upon shifting of fluorescence emission from blue to red end of the spectrum, the absorption band also shifts to the higher wavelength, this may be due to the decreasing band gap of the CuNCs from blue to orange-red. Apart from that, it can be said that the cyan emitting CuNC may be a mixture of two species with distinct absorption nature, as we found two breaks in the absorption tail.

Fluorescent emission studies

Fascinating fluorescence properties are the central attraction of metal nanoclusters. Distinct blue, cyan, green and orange-red fluorescence were observed when as-synthesized CuNCs were illuminated with an UV torch of 365 nm emission (Figure 1). The emission and excitation spectra for blue, green and orange-red CuNCs are given in Figure 2. The blue fluorescent cluster shows excitation maxima at 373 nm for the emission maxima at 450 nm with 77 nm of Stokes shift, and the corresponding quantum yield is 1.24% (with respect to quinine sulfate). The cyan emitting CuNC shows different features compared to the other cluster species; in its fluorescence emission spectrum two peaks were observed, an excitation-dependent emission peak appears at 426 to 457 nm range with respect to

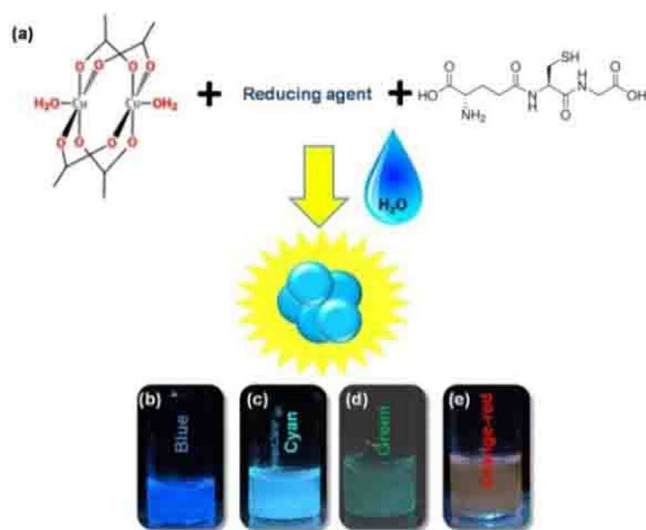


Figure 1. (a) Broad synthetic scheme of CuNCs from precursors; (b) blue, (c) cyan, (d) green and (e) orange-red emitting CuNC solutions in their respective vials.

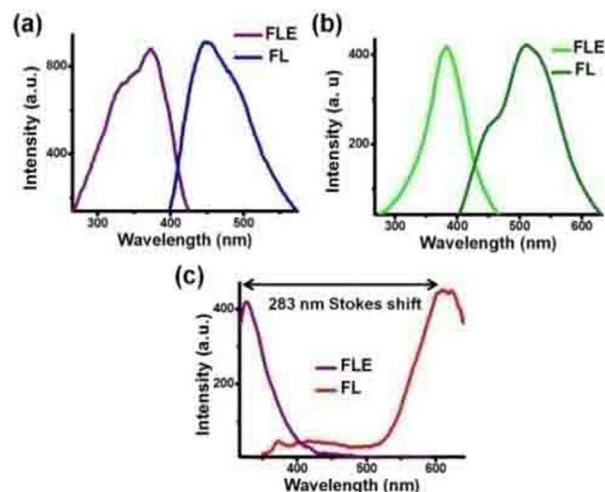


Figure 2. Fluorescence emission and excitation spectra of (a) blue, (b) green and (c) orange-red CuNCs. Orange-red clusters show a high Stokes shift of 283 nm marked by the double-headed arrow.

a change of excitation wavelength from 340 to 390 nm, and another peak at 488 nm appears for an excitation at 377 nm wavelength (with 111 nm Stokes shift) (Figure S2 of Supporting Information). This kind of excitation-dependent emission may have been originated from the structural heterogeneity of the particular fluorophore.^[16] Two peaks at the fluorescence emission spectra may appear due to presence of two distinct species present in the nanocluster solution. Fluorescence quantum yield for the cyan CuNC was found to be 1.27% (with respect to quinine sulfate). The green cluster shows strong emission maxima at 510 nm with a shoulder at 454 nm and a sharp excitation peak at 383 nm with a Stokes shift of 127 nm. The corresponding fluorescent quantum yield is 0.438% (measured with respect to atto-520 dye). The orange-red fluorescent cluster shows the most interesting behavior in the series. The fluorescence spectra of this CuNC show excitation peak at 330 nm for an emission peak at 613 nm, with a huge Stokes shift of 283 nm (Figure 2c). Such a large shift is not very common for CuNCs. Generally, fluorophores with large Stokes shift are important in cell imaging^[17] particularly in stimulated emission depletion (STED) microscopy,^[12] because selective excitation of the fluorophore is required at the expense of other fluorophores already present inside the cell. This comes from the fact that most of the fluorophores present inside the cell excite at a much higher wavelength than the clusters reported in this study. Thus, this CuNC can be utilized as a potential fluorescent agent in fluorescence microscopy.

TCSPC study

Dynamic behavior and corresponding average lifetimes of these nanoclusters at their respective fluorescent excited states were revealed from the time correlated single photon correlation (TCSPC) study. The decay profiles and corresponding time component analysis are given in Figure S3 of Supporting Information and Table 1 of main text. Both blue and green fluorescent CuNCs show three-component relaxations. For blue

Type of cluster	τ_1 (% of contribution)	τ_2 (% of contribution)	τ_3 (% of contribution)	Average lifetime
Blue	2.7 ns (51.9%)	5.4 ns (22%)	65.7 ps (25.9%)	2.62 ns
Cyan excitation at 340 nm	1.9 ns (36.3%)	3.8 ns (11.4%)	7.6 ns (52.2%)	5.11 ns
Cyan excitation at 375 nm	1.1 ns (43.4%)	4.2 ns (56.59%)	–	2.89 ns
Green	2 ns (25.3%)	8.4 ns (16.1%)	287 ps (58.4%)	2.04 ns

fluorescent CuNCs the time components are 2.7 ns (51.9%), 5.4 ns (22%) and 65.7 ps (25.9%) with an average lifetime of 2.62 ns, whereas for green clusters the relaxation components are 2.0 ns (25.3%), 8.428 ns (16.1%) and 287 ps (58.4%) with average lifetime of 2.04 ns. Interestingly, cyan emitting CuNC shows not only different relaxation times but also it shows different decay behavior, when it is excited at two different excitation wavelengths. Excitation at 340 nm leads to a three component decay profile with lifetimes 1.9 ns (36.3%), 3.81 ns (11.4%) and 7.63 ns (52.2%), with an average lifetime of 5.11 ns, whereas excitation at 375 nm leads to a two component decay process with lifetimes 1.13 ns (43.4%) and 4.24 ns (56.5%) with average life time of 2.89 ns. This result may appear due to presence of two different species in the cyan emitting CuNCs.

MALDI mass analysis

Matrix-assisted laser desorption ionization-time of flight (MALDI-TOF) mass spectrometry is an efficient technique to determine molecular weight of metal nanoclusters.^[18] Thus, it was employed to gain knowledge about the number of metal atoms in the core as well as number of ligands in the outer shell. Metal NCs are molecule-like species and from MALDI-TOF we got the molecular formula of the nanoclusters from which previous fluorescence and absorbance data can be correlated. For all types of CuNCs, positive ion mode was used and sinapinic acid was used as matrix. The optimized cluster-to-matrix ratio was 1:5 for best reproducible results in all cases (Figure 3). Blue CuNC shows peaks at m/z 522.7, 536.1, 537.1 and 538.1 corresponding to $[\text{Cu}_3(\text{GS}) + \text{Na} + 4\text{H}]^+$, $[\text{Cu}_3(\text{GS}) + \text{K} + 2\text{H}]^+$, $[\text{Cu}_3(\text{GS}) + \text{K} + 3\text{H}]^+$ and $[\text{Cu}_3(\text{GS}) + \text{K} + 4\text{H}]^+$ respectively, (GS stands for deprotonated glutathione molecule). For cyan CuNC, two species were found from MALDI-TOF analysis. Peaks at m/z 1538.1, 1558.7, 1574.9 and 1598.1 correspond to $[\text{Cu}_5(\text{GS})_5 + \text{H}]^+$, $[\text{Cu}_5(\text{GS})_5 + \text{Na}]^+$, $[\text{Cu}_5(\text{GS})_5 + \text{K}]^+$, and $[\text{Cu}_5(\text{GS})_5 + \text{Na} + \text{K}]^+$, whereas peaks at m/z 2139.2 and 2162.2 correspond to $[\text{Cu}_9(\text{GS})_5 + \text{K}]^+$ and $[\text{Cu}_9(\text{GS})_5 + \text{Na} + \text{K}]^+$. Green emitting CuNC shows peaks at m/z 3346.8 and 3491.8 corresponding to $[\text{Cu}_{10}(\text{GS})_9 + \text{Na} + \text{K}]^+$ and $[\text{Cu}_{10}(\text{GS})_9 + 3\text{Na} + \text{K}]^+$ species, whereas orange-red emitting CuNC shows one sharp peak for

m/z at 4823.33 corresponding to $[\text{Cu}_{13}(\text{GS})_{13} + \text{Na} + 3\text{H}]^+$ species. Correlating UV/Vis absorption, fluorescence data including TCSPC and MALDI-TOF analysis it can be stated that with an increase in emission wavelength, the size of the respective clusters are also increasing. With an increase in size more energy levels are added to the ground and excited states and the emission gap decreases gradually leading to red shifted fluorescent peaks.

Field emission gun-transmission electron microscopy (FEG-TEM) study

FEG-TEM of CuNCs were done to get an idea about dimensions of these tiny NCs. FEG-TEM studies of blue CuNCs (Figure 4) demonstrate that most of the blue CuNCs have a size of 1.7 nm (Figure 4). This value is comparable with the size of CuNCs reported previously by other research groups.^[5f,7a,10a,15] It has also been shown from theoretical study that copper nanoclusters show drastic variation in band gap within the size limit 2–6 nm (typical behavior of quantum dots) and above 12 nm they behave like bulk copper.^[19] The relatively larger particles are also present, and this is can be due to the aggregation of small particles protected with organic stabilizing agent.^[11] It has been documented from previous literature that

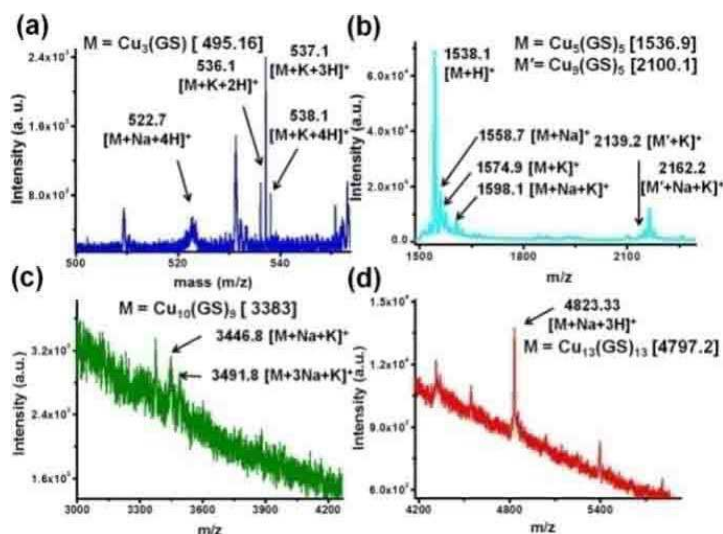


Figure 3. MALDI-TOF mass spectra of (a) blue, (b) cyan, (c) green and (d) orange-red CuNCs.

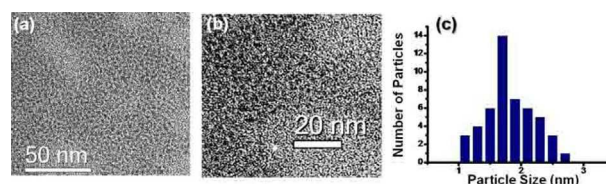


Figure 4. (a) FEG-TEM image of blue copper nanoclusters. (b) Zoom in view of the same CuNC. (c) Particle size distribution of the cluster showing the sizes from 1.1 nm to 2.7 nm with majority of the clusters centered around a size of \approx 1.7 nm.

upon the irradiation of electron beam during TEM experiments of metal nanoclusters, there is a high chance of coagulation of nanoclusters to form bigger particles.^[20,1] Sometimes strong electron beam causes destruction of organic stabilizing agents around nanoclusters and this results in coagulation of naked particles to relatively larger sized nanoparticles visible through TEM images.^[21]

X-Ray photoelectron spectroscopy (XPS) studies

To get information about valence state and bonding characteristics of metal nanoclusters X-ray photoelectron spectroscopy (XPS) is very precise and sophisticated tool of investigation. XPS data of the orange-red CuNC (Figure 5) demonstrates the

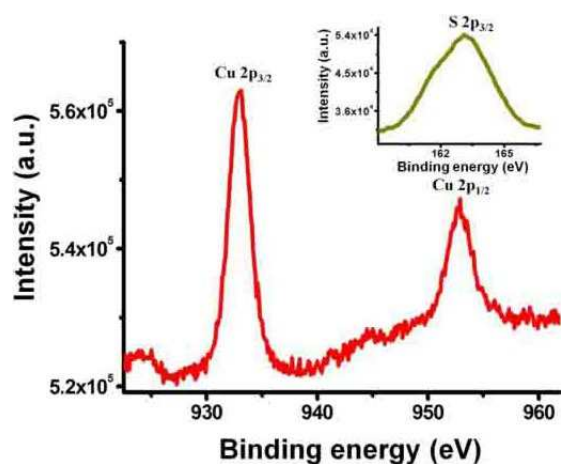


Figure 5. X-ray photoelectron spectra of orange-red CuNC showing $2p_{3/2}$ and $2p_{1/2}$ states for Cu^0 and $2p_{3/2}$ for chemisorbed S (inset).

presence of two peaks at 952.3 eV and 932.6 eV, which are characteristic peaks for $\text{Cu } 2p_{1/2}$ and $2p_{3/2}$ states of Cu^0 and Cu^I metal. No peak was found at 942 eV, confirming the absence of Cu^{2+} ions in the corresponding nanocluster. On the other hand in the binding energy range 160–166 eV range a broad peak appears at 163 eV which is the characteristic peak of sulfur (S) $2p_{3/2}$ state (inset of Figure 5 inset), indicates the presence of chemisorbed sulfur on Cu^0 surface.^[7]

FT-IR study

Fourier transform infrared (FT-IR) spectroscopic study of the dried orange-red CuNC and free glutathione was also done, which confirmed the absence of the characteristic –SH peak at 2530 cm^{-1} for the orange red CuNC, which is prominent for the corresponding free glutathione (Figure S4 of Supporting Information). This observation clearly suggests the participation of sulfur of glutathione in stabilization of nanoclusters. So it can be confirmed from the above XPS and FT-IR study that the sulfur atom of the glutathione has a direct linkage with copper atoms within the nanocluster molecules which protects the NCs from further coagulation leading to larger Cu nanoparticles.

Cytotoxicity and cell imaging studies

So far we have characterized different CuNCs to investigate their size, shape and photophysical features thoroughly. Apart from structural aspects, nanoclusters are important bioimaging tools for future applications due to their less toxicity and high photostability. It should be noted that orange-red CuNC shows a large Stokes shift of 283 nm which is very important for fluorescent microscopy (already discussed previously). These observations prompted us to explore the possibility of using the orange-red emitting nanocluster for imaging a cell line. The cytotoxicity of the nanocluster was first checked by 3-(4,5-dimethylthiazol-2-yl)-2,5-diphenyltetrazolium bromide (MTT) assay on ovarian cancerous cell line OAW42 by treating with orange-red emitting CuNC, at different concentrations. Figure 6a

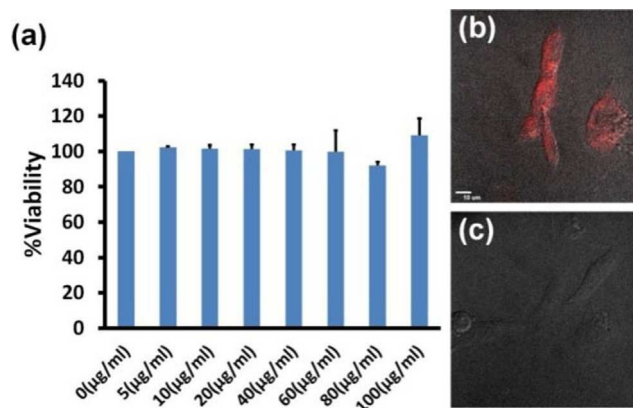


Figure 6. (a) Cytotoxicity study of the orange-red emitting CuNCs by MTT assay (OAW42 cell line), (b) confocal microscopic images of the cells treated with orange-red emitting CuNCs at a concentration $20 \mu\text{g mL}^{-1}$ and (c) control experiment without CuNCs.

shows almost 100% cell viability over a range of 0–100 $\mu\text{g mL}^{-1}$ concentration of CuNC, that is, they are almost noncytotoxic for the OAW42 cell line over an extended range of concentrations and they can be safely used as a bio-imaging substance for the corresponding cell line. Prior to treatment, the cells were serum starved and CuNC with a concentration of $20 \mu\text{g mL}^{-1}$ was added and the cells were incubated for 24 h in a 5% CO_2 incubator at 37°C . At the end of the incubation period, the medium was removed and the cells were washed in phosphate buffer saline (PBS) before fixation with 4% paraformaldehyde. The coverslips containing the cells were then mounted on a slide and sealed and imaged in a confocal microscope. Fluorescence confocal microscopy shows successful internalization of the NCs inside the cells (Figure 6b) compared to untreated cells (Figure 6c). The CuNC was synthesized in a phosphate buffer media of physiological pH (7.46) and it is quite stable inside the cell for a week as checked by fluorescence microscopy.

Photostability study of orange-red CuNC

In our current work the orange-red CuNC has been employed for cell imaging. Therefore, it is important to check the photo-

stability of the CuNC. Orange-red CuNC has an excitation maxima at 330 nm. Therefore, this nanocluster solution was exposed to a UV-source with a broad wavelength range (maxima around 360 nm). The fluorescence intensity of the nanoclusters solutions was measured from time to time to examine the effect of photoirradiation on nanocluster solution and also to check its photostability towards UV-irradiation. It has been observed that, orange-red nanoclusters do not show any significant degradation even after UV light exposure ($\lambda_{\text{max}}=360$ nm) for 3 hours. It is evident that 98% of retention of fluorescence intensity is found compared to that of initial intensity (before irradiation) of the same nanocluster solutions. So, it can be stated that this orange-red nanocluster is quite photostable. Therefore, it is expected that, these nanoclusters do not have any phototoxic effect during the timescale of cell imaging. Figure S5 in the Supporting Information illustrates the experimental results (Figure S5a to d) and photostability assay shown by the bar diagram (Figure S5e).

Conclusions

Thus, in summary, this study convincingly demonstrates a nice example of fluorescent color tuning of the CuNCs from blue to orange-red in an environmentally friendly medium (water) in presence of naturally occurring bioactive peptide. Different color emitting CuNCs with various sizes have been synthesized from the same copper precursor and stabilizing agent in aqueous medium by varying the reaction conditions and the reducing agents. Importantly, the orange-red emitting cluster has been used for imaging human ovarian cancer cell line OAW42. Moreover, the very high Stokes shift and noncytotoxic behavior of the orange-red cluster indicates its immense potential for application in real systems.

Experimental Section

Synthesis of CuNCs: All CuNCs were synthesized in aqueous medium at neutral pH or pH 7.46 (using phosphate buffer solution). Blue, cyan and green clusters were synthesized in neutral aqueous medium and orange-red cluster was synthesized at pH 7.46. In all cases metal precursor was copper acetate monohydrate $[\text{Cu}(\text{OAc})_2 \cdot \text{H}_2\text{O}]$ and for stabilizing the nanoclusters reduced glutathione (GSH) was used (see Table S1 of Supporting Information).

Synthesis of blue CuNCs: 15 mg (0.04 mmol) of reduced glutathione (GSH) and 4 mg (0.02 mmol) of copper acetate monohydrate were dissolved in 2 mL of Milli-Q water and mixed together in a round bottom flask. Then the solution was stirred at room temperature for 1 h. The round bottomed flask was then fitted with a bulb condenser and the reaction environment was made inert with nitrogen. The total set up was immersed in an oil bath with vigorous stirring at fixed bath temperature of 140 °C. After 30 min, 2 mg NaBH_4 (0.05 mmol) dissolved in 1 mL water was injected to the reaction mixture in a drop wise manner. After 8 h the reaction mixture was removed from the oil bath to get an almost colorless solution which shows blue light irradiation under UV-lamp illuminating at 365 nm.

Synthesis of cyan CuNC: 4 mg (0.02 mmol) copper acetate monohydrate, 15 mg (0.02 mmol) GSH and 4 mg (0.015 mmol) trisodium

citrate were dissolved in 2 mL, 2 mL and 1 mL Milli-Q water, respectively. Then they were mixed together in a round bottomed flask fitted with bulb condenser under nitrogenous atmosphere and stirred at 140 °C for 20 hours to get a colorless solution. The solution shows a bluish green or cyan fluorescence on UV-light irradiation of 365 nm wavelength.

Synthesis of green CuNC: 4 mg (0.02 mmol) copper acetate monohydrate, 5 mg (0.016 mmol) of GSH and 5 mg of ascorbic acid (0.028 mmol) were dissolved in 2 mL, 2 mL and 1 mL Milli-Q water, respectively. Then they were taken in a round bottomed flask and stirred for 5 minutes. The round bottomed flask was then fitted with bulb condenser at nitrogen atmosphere and heated at 120 °C for 7 hours to get a pale yellow solution which shows green fluorescence on UV lamp irradiation of 365 nm.

Synthesis of red CuNC: 4 mg (0.02 mg) copper acetate monohydrate and 15 mg (0.02 mmol) of GSH were dissolved in 2 mL Milli-Q water, and 2 mL of 50 mM phosphate buffer solution of pH 7.46 respectively. Then both were mixed in a small round bottomed flask fitted with nitrogen atmosphere and the solution was kept at 4 °C temperature in ice bath. Then 2 mg of NaBH_4 (0.05 mmol) dissolved in 1 mL Milli-Q water was added to the reaction mixture in a very slow manner for about 1 hour. Then the whole system was kept in an ice bath for the next 1 hour. An orange-red fluorescence shown on 365 nm irradiation confirms the end of the reaction.

UV/Vis spectroscopic analysis: Cary Varian 50 scan UV/Vis optical spectrometer equipped with "Cary Win" UV software was used to elucidate the optical properties of CuNCs.

Fluorescence spectroscopy: Fluorescence studies of CuNCs in a sealed cuvette were carried out in a PerkinElmer LS55 Fluorescence Spectrometer instrument. All the experiments were carried out with the excitation slit width 5 nm and emission slit width 5 nm.

Time-correlated single photon counting (TCSPC) study: TCSPC measurements were performed by means of Horiba Jobin Yvon IBH having MCP PMT Hamamatsu R3809 detector instrument and all data were fitted using Data Station v2.3. We have used NANO-LED source for excitation of samples at 340 nm and LASER source for excitation of samples at 440 nm.

MALDI-TOF MS study: The MALDI-TOF MS analyses were done using Bruker Daltonics flex Analysis mass spectrometer.

FE-TEM study: TEM study of the blue and green clusters were carried out in a JEOL 2100 KeV Ultra High Resolution Field Emission Gun (UHR FEG) TEM with voltage 200 KeV, using carbon coated copper grids.

FT-IR study: The FT-IR spectra were taken by using Shimadzu (Japan) model FT-IR spectrophotometer. In the solid state FT-IR studies, dried powder of red CuNC was mixed with KBr for preparing thin films.

X-ray photoelectron spectroscopic (XPS) study: XPS analysis of dried orange-red emitting CuNC was carried out by using an X-ray photoelectron spectroscopic (XPS, Omicron, model: 1712-62-11) method. Measurement was done by using an $\text{Al}_{K\alpha}$ radiation source under 15 kV voltages and 5 mA current.

Cytotoxicity and cell imaging studies: The cytotoxicity of the orange-red nanocluster was first checked by 3-(4, 5-dimethylthiazol-2-yl)-2,5-diphenyltetrazolium bromide (MTT) assay on ovarian cancerous cell line OAW42 by treating with orange-red emitting CuNC, at different concentrations. The cells were seeded onto 96-well plates at a density of 104 cells mL^{-1} of medium. After 24 h, the cells were serum starved and treated with different concentrations of CuNCs. 24 h post treatment, 10 μL of 3-(4, 5-dimethylthiazol-2-yl)-2, 5-diphenyltetrazolium bromide (MTT) was added per well and incubated for 3–4 h. Dimethyl sulphoxide (DMSO) was added to

stop the reaction. The optical density was measured colorimetrically at 490 nm in an ELISA reader.

For cell imaging studies the same cell line was treated with the orange-red emitting CuNC. Prior to treatment, the cells were serum starved and the CuNC with a concentration of 20 $\mu\text{g mL}^{-1}$ was added and the cells were incubated for 24 h in a 5% CO_2 incubator at 37 °C. At the end of the incubation period, the medium was removed and the cells were washed in phosphate buffer saline (PBS) before fixation with 4% paraformaldehyde. The coverslips containing the cells were then mounted on a slide and sealed and imaged in a confocal microscope.

Acknowledgements

K. Basu, K. Gayen and T. Mitra gratefully acknowledge CSIR, New Delhi (India) for doctoral fellowship. A. Baral gratefully acknowledges IACS for fellowship. S. S. Roy acknowledges CSIR for funding supports.

Conflict of interest

The authors declare no conflict of interest.

Keywords: bioimaging · cell imaging · copper nanoclusters · Stokes shift · tunable emission

- [1] a) A. Das, T. Li, G. Li, K. Nobusada, C. Zeng, N. L. Rosi, R. Jin, *Nanoscale* **2014**, *6*, 6458–6462; b) I. Díez, R. H. A. Ras, *Nanoscale* **2011**, *3*, 1963–1970; c) A. Ghosh, J. Hassinen, P. Pulkkinen, H. Tenhu, R. H. A. Ras, T. Pradeep, *Anal. Chem.* **2014**, *86*, 12185–12190; d) N. Van Steerteghem, S. V. Cleuvenbergen, S. Deckers, C. Kumara, A. Dass, H. Häkkinen, K. Clays, T. Verbiest, S. Knoppe, *Nanoscale* **2016**, *8*, 12123–12127; e) L. Shang, G. U. Nienhaus, *Int. J. Biochem. Cell Biol.* **2016**, *75*, 175–179; f) L. Yang, L. Shang, G. U. Nienhaus, *Nanoscale* **2013**, *5*, 1537–1543; g) T. J. van Wijngaarden, O. Toikkanen, P. Liljeroth, B. M. Quinn, A. Meijerink, *J. Phys. Chem. C* **2010**, *114*, 16025–16028; h) B. H. Xu, K. S. Suslick, *Adv. Mater.* **2010**, *22*, 1078–1082; i) S. Roy, A. Baral, R. Bhattacharjee, B. Jana, A. Datta, S. Ghosh, A. Banerjee, *Nanoscale* **2015**, *7*, 1912–1920; j) S. Roy, G. Palui, A. Banerjee, *Nanoscale* **2012**, *4*, 2734–2740; k) S. Choi, J. Yu, S. A. Patel, Y.-L. Tzeng, R. M. Dickson, *Photochem. Photobiol. Sci.* **2011**, *10*, 109–115; l) S. A. Patel, M. Cozzuol, J. M. Hales, C. I. Richards, M. Sartin, J.-C. Hsiang, T. Vosch, J. W. Perry, R. M. Dickson, *J. Phys. Chem. C* **2009**, *113*, 20264–20270; m) Z. Yuan, C.-C. Hu, H.-T. Chang, C. Lu, *Analyst* **2016**, *141*, 1611–1626; n) L.-Y. Chen, C.-W. Wang, Z. Yuan, H.-T. Chang, *Anal. Chem.* **2015**, *87*, 216–229; o) N. Goswami, Q. Yao, Z. Luo, J. Li, T. Chen, J. Xie, *J. Phys. Chem. Lett.* **2016**, *7*, 962–975; p) M. Iwasaki, N. Kobayashi, Y. Shichibu, K. Konishi, *Phys. Chem. Chem. Phys.* **2016**, *18*, 19433–19439; q) K. G. Stamplecoskie, Y. Chen, P. V. Kamat, *J. Phys. Chem. C* **2014**, *118*, 1370–1376; r) K. G. Stamplecoskie, P. V. Kamat, *J. Phys. Chem. Lett.* **2015**, *6*, 1870–1875; s) A. Baksi, P. Chakraborty, S. Bhat, A. Natarajan, T. Pradeep, *Chem. Commun.* **2016**, *52*, 8397–8400; t) C. Zeng, Y. Chen, K. Iida, K. Nobusada, K. Kirschbaum, K. J. Lambright, R. Jin, *J. Am. Chem. Soc.* **2016**, *138*, 3950–3953; u) V. Jeseentharani, N. Pugazhenthiran, A. Mathew, I. Chakraborty, A. Baksi, J. Ghosh, M. Jash, G. S. Anjusree, T. G. Deepak, A. S. Nair, T. Pradeep, *ChemistrySelect* **2017**, *2*, 1454–1463; v) Y. Lu, W. Chen, *Chem. Soc. Rev.* **2012**, *41*, 3594–3623.
- [2] R. Ghosh, U. Goswami, S. S. Ghosh, A. Paul, A. Chattopadhyay, *ACS Appl. Mater. Interfaces* **2015**, *7*, 209–222.
- [3] D. C. Harris in *Quantitative chemical analysis, 7th ed.*, W. H. Freeman and Company, **2007**, AP20–AP27.
- [4] a) D. Cauzzi, R. Pattacini, M. Delferro, F. Dini, C. D. Natale, R. Paolesse, S. Bonacchi, M. Montalti, N. Zaccheroni, M. Calvaresi, F. Zerbetto, L. Prodi, *Angew. Chem. Int. Ed.* **2012**, *51*, 9662–9665; *Angew. Chem.* **2012**, *124*, 9800–9803; b) Z. Wu, Y. Li, J. Liu, Z. Lu, H. Zhang, B. Yang, *Angew. Chem. Int. Ed.* **2014**, *53*, 12196–12200; *Angew. Chem.* **2014**, *126*, 12392–12396; c) Y. Lin, P. Chen, Z. Yuan, J. Ma, H. Chang, *Chem. Commun.* **2015**, *51*, 11983–11986; d) H. Kawasaki, Y. Kosaka, Y. Myoujin, T. Narushima, T. Yonezawa, R. Arakawa, *Chem. Commun.* **2011**, *47*, 7740–7742; e) X. Yuan, Z. Luo, Q. Zhang, X. Zhang, Y. Zheng, J. Y. Lee, J. Xie, *ACS Nano* **2011**, *5*, 8800–8808; f) Z. Qing, X. He, D. He, K. Wang, F. Xu, T. Qing, X. Yang, *Angew. Chem. Int. Ed.* **2013**, *52*, 9719–9722; *Angew. Chem.* **2013**, *125*, 9901–9904; g) Y. Zhang, Z. Chen, Y. Tao, Z. Wang, J. Ren, X. Qu, *Chem. Commun.* **2015**, *51*, 11496–11499; h) X. Gao, C. Du, C. Zhang, W. Chen, *ChemElectroChem* **2016**, *3*, 1266–1272; i) X. Gao, S. He, C. Zhang, C. Du, X. Chen, W. Xing, S. Chen, A. Clayborne, W. Chen, *Adv. Sci.* **2016**, *3*, 1600126; j) Y.-S. Borghei, M. Hosseini, M. Khoobi, M. R. Ganjali, *J. Fluoresc.* **2017**, *27*, 529.
- [5] a) X. Jia, X. Yang, J. Li, D. Li, E. Wang, *Chem. Commun.* **2014**, *50*, 237–239; b) Z. Mao, Z. Qing, T. Qing, F. Xu, L. Wen, X. He, D. He, H. Shi, K. Wang, *Anal. Chem.* **2015**, *87*, 7454–7460; c) F. Xu, H. Shi, X. He, K. Wang, D. Wang, Q. Guo, Z. Qing, L. Yan, X. Ye, D. Li, J. Tang, *Anal. Chem.* **2014**, *86*, 6976–6982; d) Z. Qing, T. Qing, Z. Mao, X. He, K. Wang, Z. Zou, H. Shi, D. He, *Chem. Commun.* **2014**, *50*, 12746–12748; e) N. Vilar-Vidal, J. Rivas, M. A. López-Quintela, *Phys. Chem. Chem. Phys.* **2014**, *16*, 26427–26430; f) C. Wang, Y. Huang, *NANO* **2013**, *08*, 1350054; g) S. Huseynova, J. Blanco, F. G. Requejo, J. M. Ramallo-López, M. C. Blanco, D. Buceta, M. A. López-Quintela, *J. Phys. Chem. C* **2016**, *120*, 15902–15908; h) Y. Guo, F. Cao, X. Lei, L. Mang, S. Cheng, J. Song, *Nanoscale* **2016**, *8*, 4852–4863; i) N. K. Das, S. Ghosh, A. Priya, S. Datta, S. Mukherjee, *J. Phys. Chem. C* **2015**, *119*, 24657–24664.
- [6] X. Jia, J. Li, L. Han, J. Ren, X. Yang, E. Wang, *ACS Nano* **2012**, *6*, 3311–3317.
- [7] R. Ghosh, A. K. Sahoo, S. S. Ghosh, A. Paul, A. Chattopadhyay, *ACS Appl. Mater. Interfaces* **2014**, *6*, 3822–3828.
- [8] W. Wei, Y. Lu, W. Chen, S. Chen, *J. Am. Chem. Soc.* **2011**, *133*, 2060–2063.
- [9] B. Fiser, B. Jójárt, M. Szőri, G. Lendvai, I. G. Csizmadia, B. Viskolcz, *J. Phys. Chem. B* **2015**, *119*, 3940–3947.
- [10] a) X. Jia, J. Li, E. Wang, *Small* **2013**, *9*, 3873–3879; b) X. Gao, Y. Lu, M. Liu, S. He, W. Chen, *J. Mater. Chem. C* **2015**, *3*, 4050–4056.
- [11] S. Basu, S. Majumder, S. Chatterjee, A. Ganguly, T. Efferth, S. K. Choudhuri, *in vivo* **2009**, *23*, 401–408.
- [12] M. V. Sednev, V. N. Belov, S. W. Hell, *Methods Appl. Fluoresc.* **2015**, *3*, 042004.
- [13] M. A. H. Muhammed, P. K. Verma, S. K. Pal, R. C. A. Kumar, S. Paul, R. V. Omkumar, T. Pradeep, *Chem. Eur. J.* **2009**, *15*, 10110–10120.
- [14] J. Zheng, J. T. Petty, R. M. Dickson, *J. Am. Chem. Soc.* **2003**, *125*, 7780–7781.
- [15] C. Vázquez-Vázquez, M. Bañobre-López, A. Mitra, M. A. López-Quintela, J. Rivas, *Langmuir* **2009**, *25*, 8208–8216.
- [16] I. Díez, M. I. Kanyuk, A. P. Demchenko, A. Walther, H. Jiang, O. Ikkala, R. H. A. Ras, *Nanoscale* **2012**, *4*, 4434–4437.
- [17] a) X. Tu, W. Chen, X. Guo, *Nanotechnology* **2011**, *22*, 095701; b) A. C. Benniston, T. P. L. Winstanley, H. Lemmetyinen, N. V. Tkachenko, R. W. Harrington, C. W. Wills, *Org. Lett.* **2012**, *14*, 1374–1377.
- [18] Y. Lu, W. Chen, *Anal. Chem.* **2015**, *87*, 10659–10667.
- [19] P. G. Prabhaskar, S. S. Nair, *AIP Adv.* **2016**, *6*, 055003.
- [20] a) P. Ramasamy, S. Guha, E. S. Shibu, T. S. Sreeprasad, S. Bag, A. Banerjee, T. Pradeep, *J. Mater. Chem.* **2009**, *19*, 8456–8462; b) D. Stellwagen, A. Weber, G. L. Bovenkamp, R. Jin, J. H. Bitter, C. S. S. R. Kumar, *RSC Adv.* **2012**, *2*, 2276–2283.
- [21] W. D. Pyrz, D. J. Buttrey, *Langmuir* **2008**, *24*, 11350–11360.

Manuscript received: June 19, 2017

Revised manuscript received: July 28, 2017

Accepted manuscript online: August 7, 2017

Version of record online: September 5, 2017